Jurnal Teknologi

Full Paper

TAPERED ANGLE MICROFLUIDIC DEVICE FOR CELL SEPARATION USING HYDRODYNAMIC PRINCIPLE

Muhammad Asyraf Jamrus, Mohd Ridzuan Ahmad*

Department of Control and Mechatronics Engineering, Faculty of Electrical Engineering, Universiti Teknologi Malaysia, 81310 UTM Johor Bahru, Johor, Malaysia

Article history
Received
1 November 2022
Received in revised form
26 January 2024
Accepted
15 February 2024
Published Online
23 June 2024

*Corresponding author
mdridzuan@utm.my

Graphical abstract

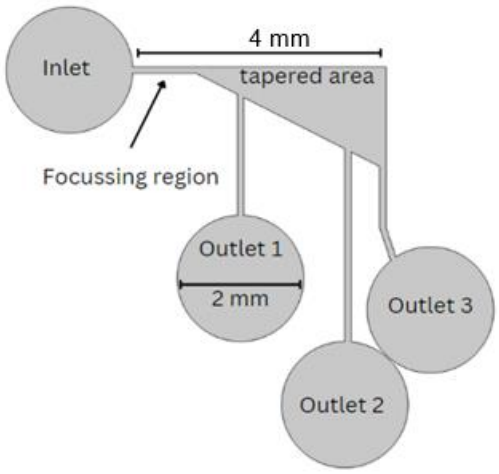

Abstract

Cell sorting is an essential technique used in a wide range of research, diagnostic, and therapeutic sectors. Fluorescence-activated cell sorting (FACS), magnetic-activated cell sorting (MACS), and CellSearch, which are conventional techniques, possess inherent limitations. For instance, the utilization of EpCam was ineffective in identifying specific malignancies. Cell sorting techniques have undergone significant advancements, with microfluidics being one of them. Regrettably, the current devices suffer from issues such as clogging and necessitate a lengthy main channel. Therefore, the goal of this work is to build and improve a microfluidic device with a tapered angle. There are three designs presented, each with one inlet, at least two exits, one focusing zone, and one tapering region. Using the finite element simulation software COMSOL Multiphysics, two studies are undertaken, the first examining the effect of taper angle on particle separation, and the second analyzing the effect of flow rate on particle separation. Based on the hydrodynamic theory and sedimentation process, this design allows particles to separate. When the taper angle approached 20 degrees, a mixture of 3 µm and 10 µm polystyrene microbeads were successfully separated, and separation continued until the taper angle approached 89 degrees. This technology offers simple, label-free, and continuous separation of many particles in a self-contained device without the use of bulky gear.

Keywords: CTC, microfluidic device, tapered angle, sedimentation process, passive separation

Abstrak

Pemisahan sel merupakan teknik penting yang digunakan dalam pelbagai bidang penyelidikan, diagnostik dan terapeutik. Pengelasan sel yang diaktifkan oleh *fluorescence* (FACS), pengelasan cell yang diaktifkan magnetik (MACS) dan *CellSearch*, yang merupakan teknik konvensional, mempunyai keterbatasan yang wujud. Sebagai contoh, penggunaan EpCam tidak berkesan dalam mengenal pasti malignansi tertentu. Teknik pemisahan sel telah mengalami kemajuan yang signifikan, dengan microfluidics menjadi salah satu daripada mereka. Malangnya, peranti semasa menderita masalah seperti kemacetan dan memerlukan saluran utama yang panjang. Oleh itu, matlamat kerja ini adalah untuk membina dan menambah baik peranti mikrobendalir dengan sudut tirus. Terdapat tiga reka bentuk yang dibentangkan, setiap satu dengan satu salur masuk, sekurang-kurangnya dua pintu keluar, satu zon fokus dan satu kawasan tirus. Menggunakan perisian simulasi unsur terhingga COMSOL Multiphysics, dua Kajian dijalankan, yang pertama mengkaji kesan sudut tirus pada

pemisahan zarah, dan yang kedua menganalisis kesan kadar aliran pada pemisahan zarah. Berdasarkan teori hidrodinamik dan proses pemendapan, reka bentuk ini membolehkan zarah-zarah berpisah. Apabila sudut tirus menghampiri 20 darjah, campuran 3 µm dan 10 µm polistirena microbeads berjaya diasingkan, dan pemisahan berterusan sehingga sudut tirus menghampiri 89 darjah. Teknologi ini menawarkan pemisahan yang mudah, bebas label dan berterusan bagi banyak zarah dalam peranti serba lengkap tanpa menggunakan gear besar.

Kata kunci: CTC, peranti mikrobendalir, sudut tirus, proses pemendapan, pemisahan pasif

1.0 INTRODUCTION

The application of cell sorting, and microfluidic techniques has had a profound impact on the fields of biology and medicine since it allows for the precise separation and investigation of targeted cell populations. Nevertheless, there are numerous obstacles linked to these methodologies. An important problem is the inadequate reporting of the rates at which conventional sorting technologies such as fluorescence-activated cell sorting (FACS) and magnetic-activated cell sorting (MACS) can process throughputs, yields, viabilities, and processing times [1]. The absence of thorough reporting impedes the capacity to efficiently compare and optimize various strategies.

Conventional cell sorting approaches have a restricted ability to uncover intricate cellular interactions, as pointed out by Nitta *et al*. [2]. In addition, the act of sorting cells might modify their redox state and cellular metabolome, leading to difficulties in properly determining the actual condition of the cells [3]. This constraint is especially noteworthy when examining cellular metabolism and its influence on cell behavior and function. Moreover, conventional cell sorting methods may not fully meet the requirements of certain applications, such as tissue engineering, where the need for quenching metabolism before cell sorting may not align with the specific needs of these advanced applications [4].

Several conventional methods are approved by the Food and Drug Administration (FDA) like CellSearch [5]. Nevertheless, it is important to carefully assess the limits of these FDA-approved treatments before applying them. A major drawback of FDA-approved CTC separation methods is their dependence on certain markers, such as EpCAM, for capturing CTCs. This methodology may fail to detect certain cancers [6]. In addition, the CellSearch method fails to identify circulating tumor cells (CTCs) in a significant number of patients with advanced metastatic illness, but a small proportion of patients exhibit exceptionally high levels of CTCs in their peripheral blood [7]. This emphasizes the necessity for enhanced sensitivity and specificity in CTC separation techniques to guarantee thorough and precise identification of CTCs among various groups of patients.

Nevertheless, cell separation techniques have undergone significant advancements over the years. Several techniques have been devised for cell separation, with one such way being microfluidic. Microfluidics involves the manipulation of fluids at the microscale level. It has found applications in various areas such as high-precision materials synthesis, biochemical sample preparation, biophysical analysis, medical diagnostics, and drug development [8,9]. The technology has gained significant attention in research fields including nanotechnology, materials science, medicine, bioengineering, and chemistry [10-12]. The technology enables the precise handling of small amounts of fluids, typically in the range of nanoliters to microliters, and offers advantages such as high throughput, reduced reagent consumption, and improved reproducibility [13,14].

The application of these technologies in the detection and isolation of cancer cells has been widely utilized, highlighting their importance in the advancement of healthcare and medical research [15]. In addition, microfluidic technologies provide rapid and precise separation of intricate samples, resulting in a high level of separation accuracy [16, 17] [32, 33]. This study will specifically concentrate on passive separation, which is one of the two categories of microfluidic separation techniques.

Passive separation techniques utilize microfluidic processes and the interaction between fluids and the device's geometry to produce separation, as explained in the description [18]. These methods rely on the natural behavior of fluids, such as inertial forces, hydrodynamic effects, and surface interactions, to drive the separation process. These techniques are preferred for their simplicity, ease of fabrication, and portability, making them suitable for various applications, including plasma separation, cell sorting, and biomarker detection [19-21]. Passive microfluidic devices are widely recognized for their ability to handle large amounts of samples and are commonly used in biomedical and clinical environments because of their user-friendly characteristics and seamless integration into diagnostic platforms [22-24].

Deterministic Lateral Displacement (DLD), Inertial microfluidic, and Hydrodynamic Filtration are some of the popular devices that are used in cell sorting. These devices are simple, low-cost, and robust separation of various biological and non-biological entities [25, 26]. While passive separation devices offer numerous advantages, they also have limitations. A major drawback of passive separation microfluidic techniques is their limited throughput, which is primarily constrained by the requirement to maintain force equilibrium at low Reynolds number flows during microfluidic separations [27]. In addition, current passive microfluidic techniques frequently necessitate lengthy channel dimensions, demand the use of labeling procedures, and experience limitations in terms of throughput [28]. The constraints impede the practical use of passive separation microfluidic techniques in high-throughput environments and may limit their efficacy in specific separation jobs. Moreover, the need for extended channel lengths in current passive microfluidic techniques may present practical constraints in specific applications, particularly when small and effective separation devices are sought after [29].

This work presents a proposed design of a tapered-angle passive microfluidic device for cell sorting, which incorporates the hydrodynamic principle.

2.0 THEORY

2.1 Working Principle

The proposed microfluidic design consists of one inlet, three outlets, one focusing region, and a tapered area ranging from 6 to 65 degrees angle. The inlet and outlet diameter are fixed at 2mm while the focusing region length is 1mm. The schematic of the proposed design is shown in Figure 1.

Separating micro-objects using hydrodynamic spreading involved adjusting the hydrodynamic spreading generated by the tapered device design. A tapered microchannel is one whose width gradually increases. This unique design maximizes velocity dispersion in order to produce a pressure difference between the main channel and the three outputs. Increased velocities imply a lower hydrodynamic resistance feature, which is required for particle entrapment to occur successfully toward the appropriate outlets. Because it converged via a short focus zone, there was no need for a buffer or sheath flow. After the sample flow is delivered continuously to the inlet, the particles concentrate at the focusing zone. When particles are near the focusing region's end, they begin to follow their own trajectory, resulting in a vertical position difference between particles of different sizes. When the velocity in the tapered zone continues to decrease, gravity takes over, and sedimentation begins. Sedimentation is the separation of suspended particles in a liquid by gravity [30].

Larger particles with size-dependent trajectories were sucked into the carrier flow. Sedimentation is visible in tapered microchannels due to the minuscule dimensions used, particularly the channel height [31]. As a result, larger particles are collected at Outlet 1, while the smallest particles are collected at Outlet 3, and some particles are collected at Outlet 2.

2.2 Hydrodynamic Equations

According to Figure 2, the sample flow across a separation device can be described using an equivalent fluidic circuit with discrete resistive components R_{sense} and $R_{h1\text{-}3}$ (for the tapered region). The hydrodynamic flow resistance for incompressible Newton's fluid is given as (1):

$$\Delta P = QR_h \tag{1}$$

Where:
Q = Volumetric flow rate
ΔP = Pressure differential between the channel's outlet and inlet
R_h = Hydrodynamic resistance

The outlet with the Rh resistance has the highest velocity, which has an effect on how suspended particles migrate inside tapered microfluidics to exit by this outlet. Hydrodynamic resistance totally relies on the geometry; hence the equation can be shown as (2)(3):

$$R_{h,rect} = \frac{32\mu L}{D^2 \omega d} \tag{2}$$

$$R_{h,tapered} = \frac{12\mu L}{h^3} \frac{\ln\left(\frac{\omega_1}{\omega_0}\right)}{\omega_1 - \omega_0} \tag{3}$$

Where:
h = height
ω0,1 = width
L = linear dimension

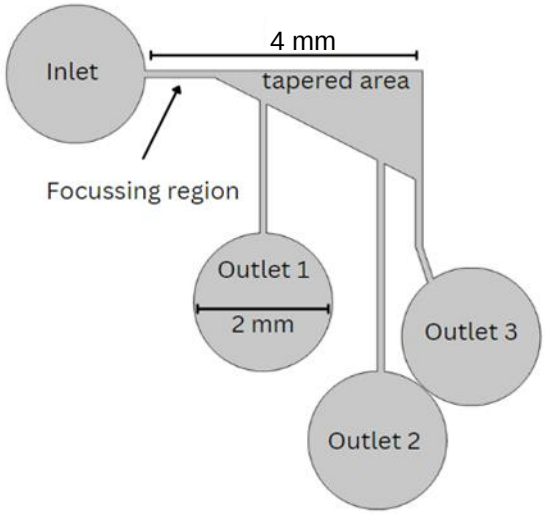

Figure 1 Schematic of the proposed design

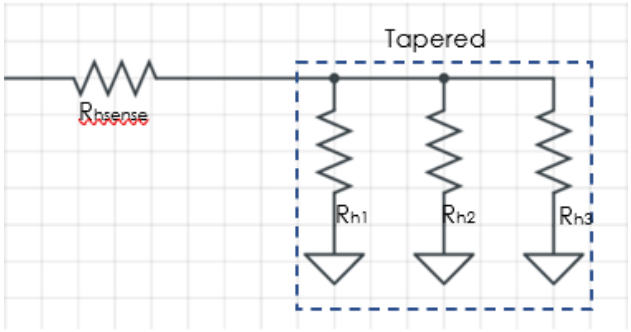

Figure 5 Tapered microfluidic equivalent fluidic circuit

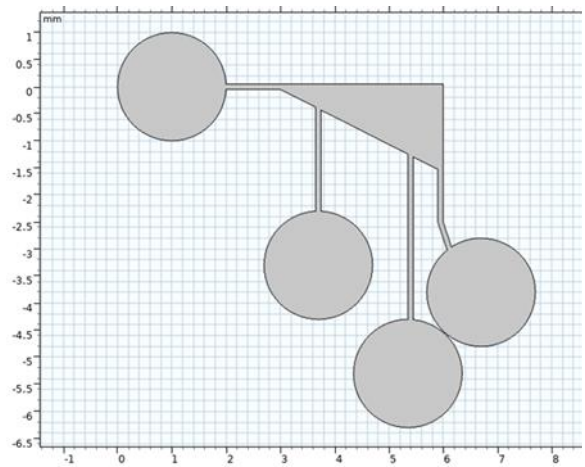

Figure 2 First proposed geometry design for tapered angle microfluidic device

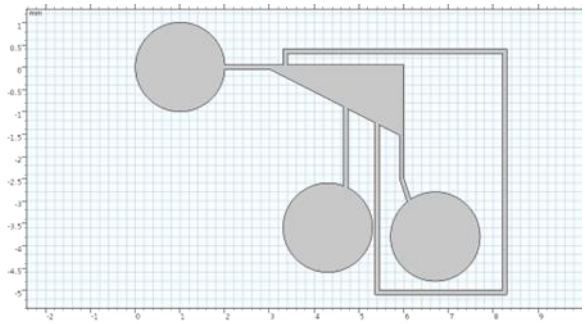

Figure 3 Second proposed geometry design for tapered angle microfluidic device

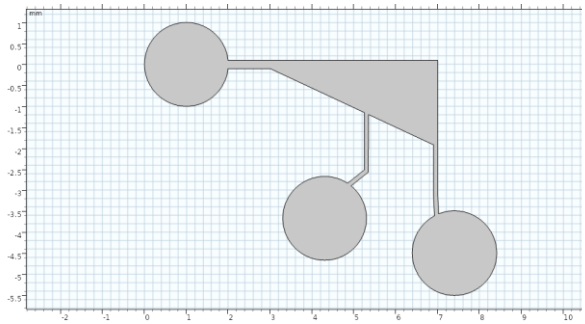

Figure 4 Third proposed geometry design for tapered angle microfluidic device

3.0 METHODOLOGY

3. Design Specifications

The tapered angle microfluidic design has one inlet and a maximum of three exits with a diameter of 2 mm, a focusing zone with a length of 1 mm and a height of 100 µm, and a tapered area. Several tapered angles have been implemented in this study to find the best angle for cell separation. With a flow rate ranging from 0.5 µL/min to 3.0 µL/min, laminar fluid flow will be supplied into the inlet.

3.2 Proposed Solution

An ideal cell separation device should have good sample purity, be cost-effective, use simple equipment, and drastically reduce the time necessary to sort a large volume of samples. As a result, the proposed design for a tapered angle microfluidic device in this work is based on the Hydrodynamic Principle and it will be described more below.

This microfluidic device is intended to feature a single inlet, a single focusing region, a single main channel, and three outlets (Figure 1). Additionally, the tapered angle will be established once the desired results have been obtained.

3.3 Tapered Angle Microfluidic Design

The tapered-angle microfluidic device was developed utilizing COMSOL Multiphysics. Figure 3 displays the first geometric design of the microfluidic device with a tapered angle. The inlet and outlet diameter are fixed at 2 mm, while the focusing zone measures 1 mm in length and 100 µm in width. The design was influenced by the work of Laila *et al* [31]. The first design incorporated multiple tapered angles. Figure 4 illustrates the proposed design, which is identical to the original concept, except that outlet 2 has been substituted with feedback. The reason for this is to prevent the accumulation of cells at outlet 2, as will be demonstrated in the results section. Figure 5. The design features dual outputs, and the focus zone is expanded by 2 mm in order to minimize cell contact.

3.4 Evaluate the Designs

In order to analyze the design, numerous COMSOL functionalities were utilized. In this study, the laminar fluid flow was applied at the inlet. Laminar fluid flow was chosen for this project because the fluid travels smoothly or in regular patterns, as opposed to turbulent flow, in which the fluid fluctuates irregularly. Using probing features, the velocity value may be obtained, and it appears that the velocity at outlet 3 is the highest, implying that it has the lowest hydrodynamic resistance compared to outlets 1 and 2. This velocity feature can be further adjusted using the hydrodynamic principle to achieve successful particle separation or particle entrapment.

Two particle trajectories were utilized to replicate the trajectory of PS microbeads with a diameter and density of 3 µm and 10 µm, 1050 kg/m^3 and 2290 kg/m^3, respectively, and these particles were discharged continuously at the inlet from 0 to 5 seconds in 0.1-second increments and the number of particles released at the inlet is random. In addition, the probe was positioned at each outlet to determine the number of particle traps at each outlet. The model is verified through a comparison with the experimental findings of Laila *et al*. [31]. configuration. The comparison is made by evaluating the purity of the cells collected at each outlet when the ideal tapering angle is achieved. Purity is the proportion of the desired target particles at a specific outlet, expressed as a percentage of all particles at the same outlet. The expression is computed for each outlet (4):

$$Purity = \frac{targeted\ cell}{targeted\ particles + unwanted\ particles} \quad (4)$$

4.0 RESULTS AND DISCUSSIONS

Three investigations were conducted in this study: the effect of tapering angle on cell separation, the effect of flow rate on cell separation, and a comparison of the three designs.

4.1 The Effect of Tapering Angle on Cell Separation

In this investigation, several tapered angles were applied with a constant flow rate of 3 µl/min to study the effect of tapering angle on cell separation. Figures 6 and 7 show how the tapered angle affects the streamline for 6 and 27 tapering angles, respectively. Meanwhile, Figure 8 depicts the particles gathered at each outlet. This is due to the Stokes number governing sedimentation inside microfluidic devices, which are heavily reliant on mass. This investigation is to determine the optimum tapered angle for the cells to separate.

In a tapered microfluidic system, the taper angle is crucial since it controls the sedimentation rate (sedimentation velocity). Consequently, it was determined that the greater the taper angle, the quicker the sedimentation. Consequently, it was determined that the greater the taper angle, the quicker the sedimentation. Figure 8 demonstrates that a mixture of PS microbeads with varying sizes and densities does not separate at taper angles of 6 and 12 degrees. This is owing to the fact that the tapering area is insufficient for sedimentation to take place.

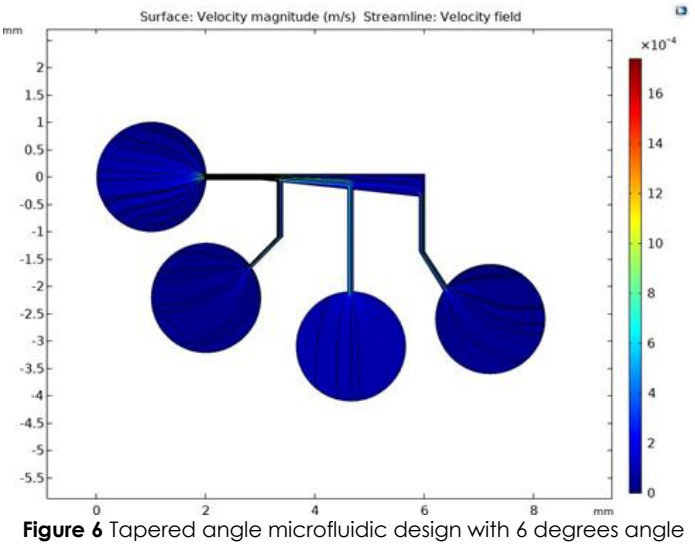

Figure 6 Tapered angle microfluidic design with 6 degrees angle

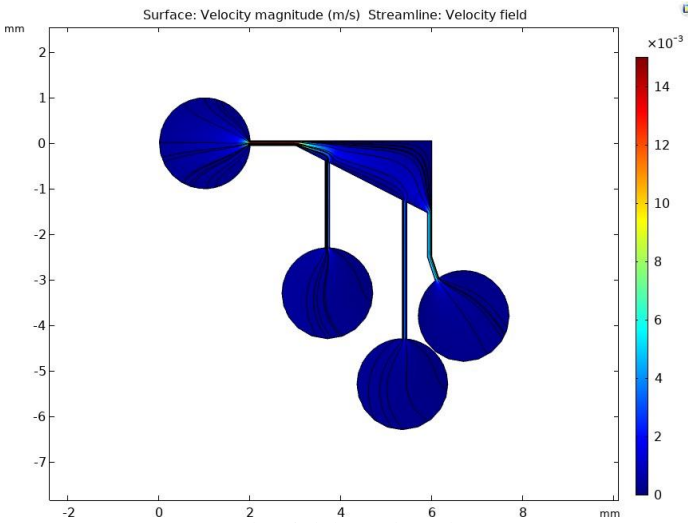

Figure 7 Tapered angle microfluidic design with 6 degrees angle

In addition, a combination of particles separates when the taper angle approaches 20 degrees, and it can continue to separate up to an angle of 65 degrees. Therefore, we can assume that separation can occur somewhere between 20 and 89 degrees of taper angle. As the angle of the taper approaches 30 degrees, however, the number of particles gathered at outlets 1 and 3 falls progressively. The optimum taper angle for cell separation is 27 degrees, with the big and small particles collected at both outlets 1 and 3 respectively.

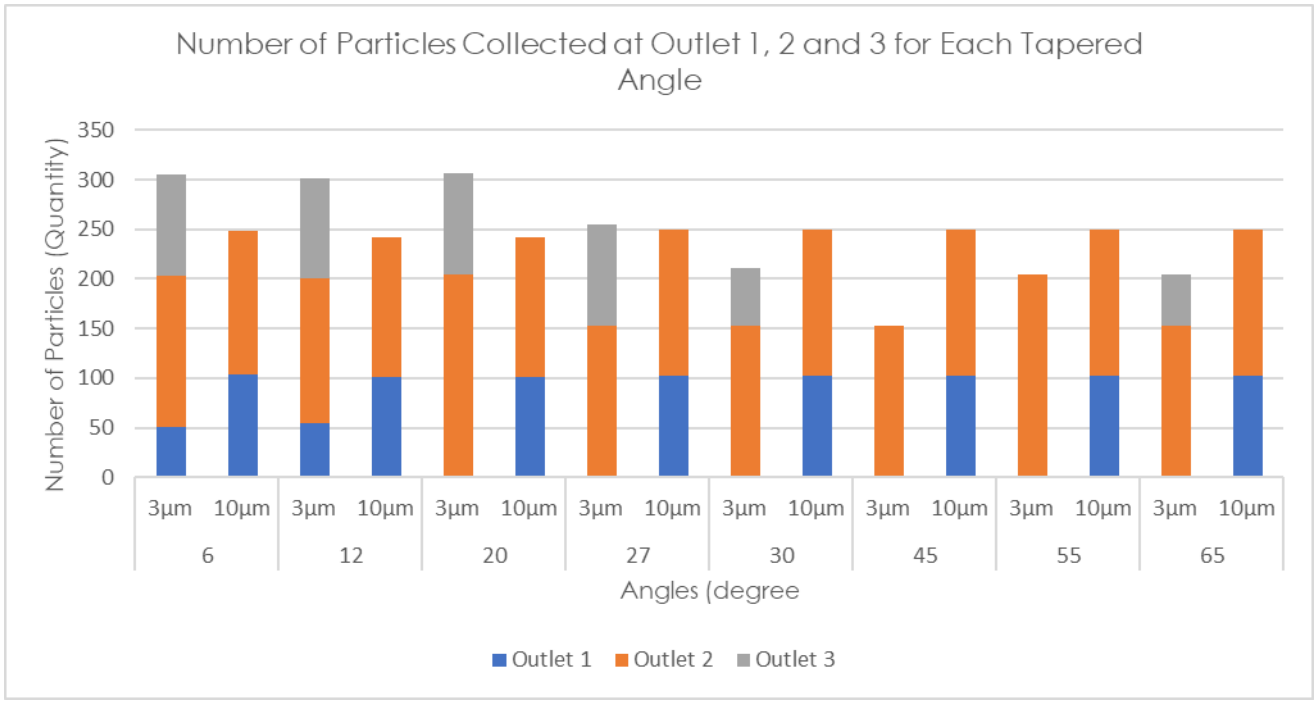

Figure 8 Particles collected on each outlet for each tapered angle

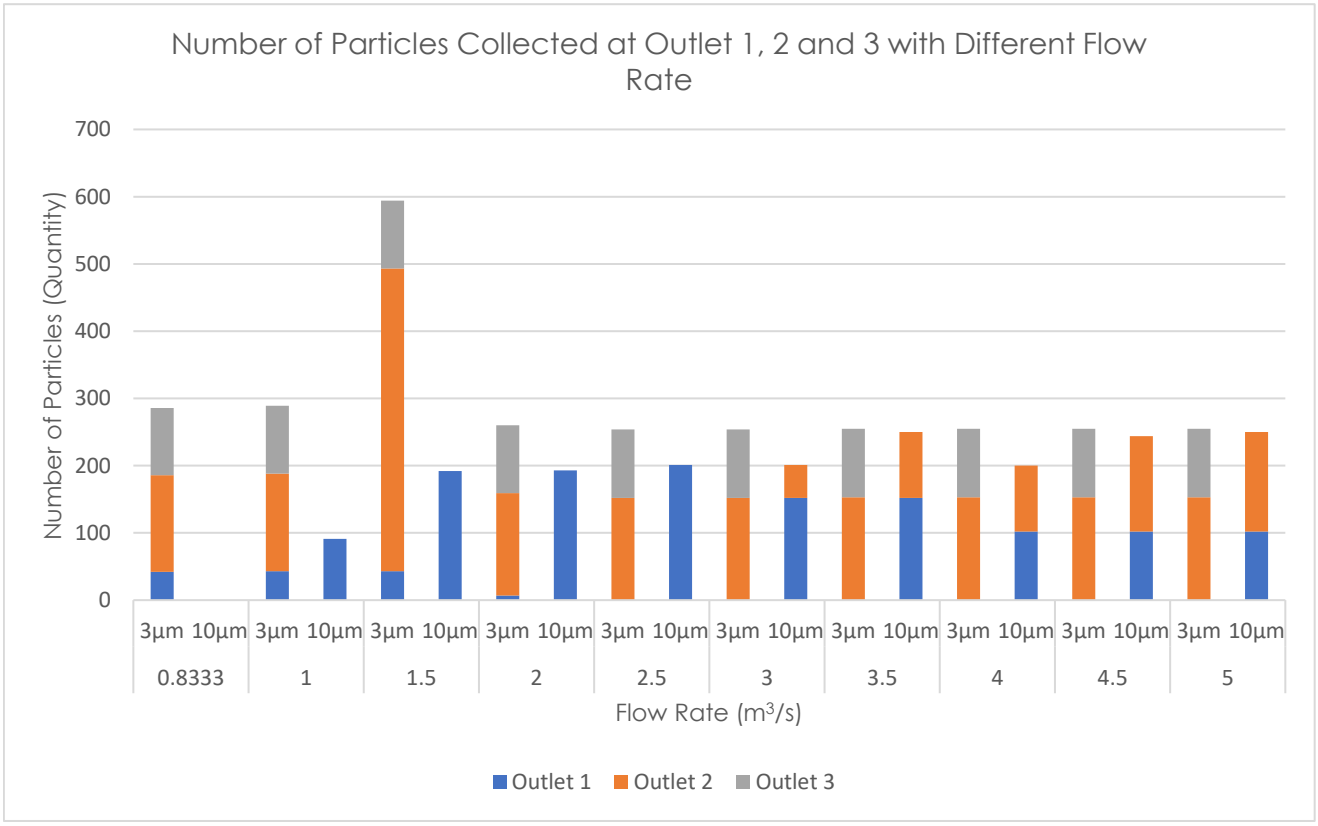

Figure 9 Particles collected on each outlet for each flow rate

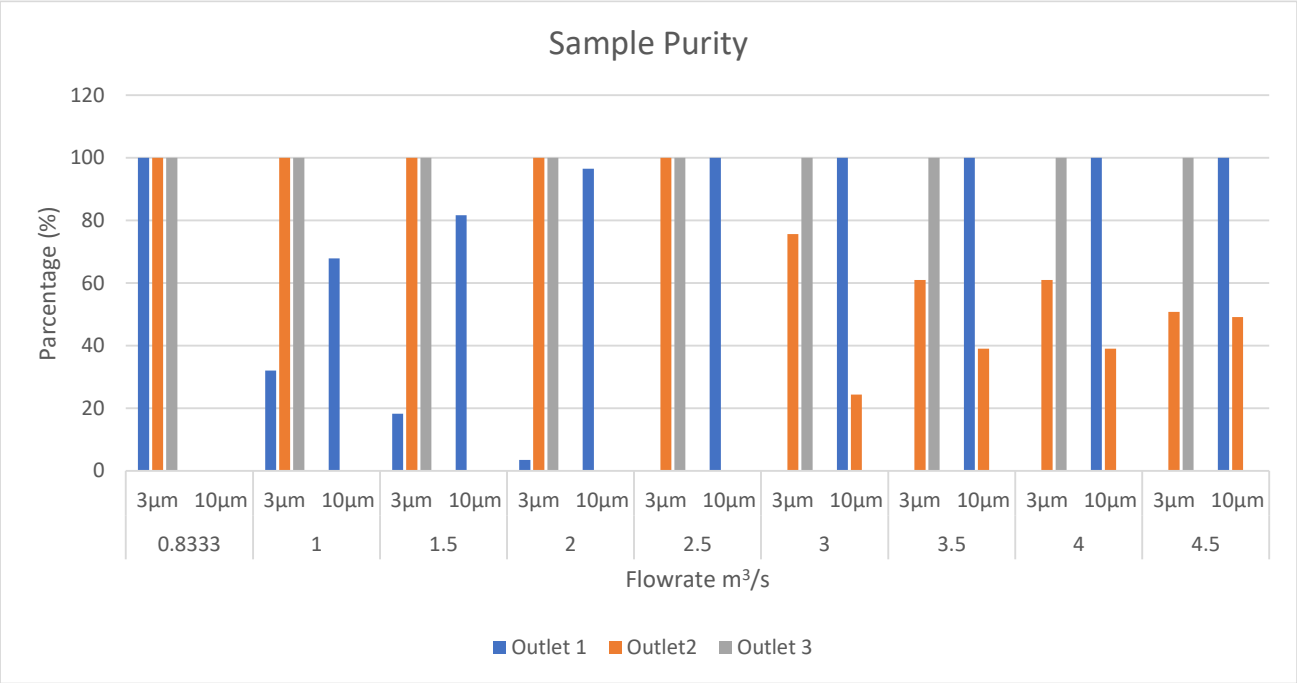

Figure 10 Sample purity of the particles at each outlet

4.2 Flow Rate's Impact on Particle Separation

In this study, the flow rate used ranges from 0.5 µl/min to 3.0 µl/min. Due to their reliance on hydrodynamic principles, these devices are extremely sensitive to the flow rates at the inlet. Lower flow rates
might result in a faster sedimentation process; as a result, particles may not be completely separated.

Conversely, lower flow rates can result in a slower sedimentation process, which may result in larger particles being trapped at the furthest outlet. Consequently, determining the optimal flow rates enables particles to follow the correct trajectory and be captured at the right outlets. Figure 9 illustrates the effect of flow rates on particle separation at the optimal taper angle (27 degrees) meanwhile Figure 10 depicts the purity of the particle at each outlet.

Based on Figure 9, at 0.8333 m^3/s, there are no large particles trapped in any outlets. This is due to the velocity is not high enough for the large particle to move through into the focusing region and taper area, resulting in the bulk of the particles stopping at the inlet and at the focusing region. Next, at 1.5 to 2 m^3/s, several small particles are trapped at outlet 1. This is because the velocity of some small particles is insufficient for further travel, which may be the result of a collision at the focusing region

Figure 10 shows that a mixture of particles started to fully separate with 100 percent sample purity at outlets 1 and 2 at a flow rate of 2.5 to 5 m^3/s. Aside from that, it appears that the quantity of larger particles trapped at outlet 1 increases as the flow rate increases until it reaches 2.5 m^3/s, after which it declines because the faster velocity of some larger particles causes a late sedimentation process to occur. The ideal flow rate based on the number of particles trapped in each outlet is 2.5 m^3/s for all larger particles captured at outlet 1, whereas small particles are trapped at outlets 2 and 3.

4.3 The Designs Comparison

In this study, three designs have been developed. The first design features one inlet, a focusing region, a 27-degree tapered area, and three outlets, while the second design is identical to the first with the exception that outlet two is connected to the tapered area. The third design is identical to the first, except that it has two outlets and the length of the tapering section and height of the focusing region are each enlarged by 1 mm. These designs are depicted in Figures 11 to 13.

Figures 11 to 13 depict the streamline inside microfluidic devices subjected to laminar flow at the entrance. Streamline is crucial since it determines the particle's path. Figures 11 and 13 illustrate the streamline traveling through each outlet, indicating that particles will accumulate at each outlet. In contrast, Figure 12 depicts the streamline going through outlets 1 and 3, but not outlet 2 (feedback), resulting in no particles being caught at outlet 2.

Figure 14 depicts a bar graph of the collected particles at each outlet for the three designs. The first design demonstrates that sample purity is 100 percent at outlets 1, 2, and 3, with large particles at outlet 1 and small particles trapped at outlets 2 and 3. This is due to the optimal angle and flow rates used.

However, the amount of gathered particles is insufficient compared to the other two designs.

The second design demonstrates that the sample purity of big particles at the first outlet is 70 percent, whereas the sample purity of the small particles at the second outlet is 100 percent. The second design's objective is to eliminate the particles trapped in outlet 2, hence feedback was employed by connecting outlet 2 to the tapered area. In addition, this design is capable of trapping a greater number of particles at each outlet than the initial design.

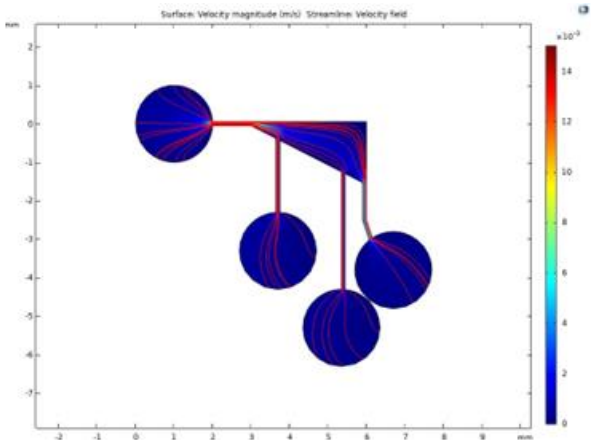

Figure 11 Streamline inside the tapered angle microfluidic for the first design

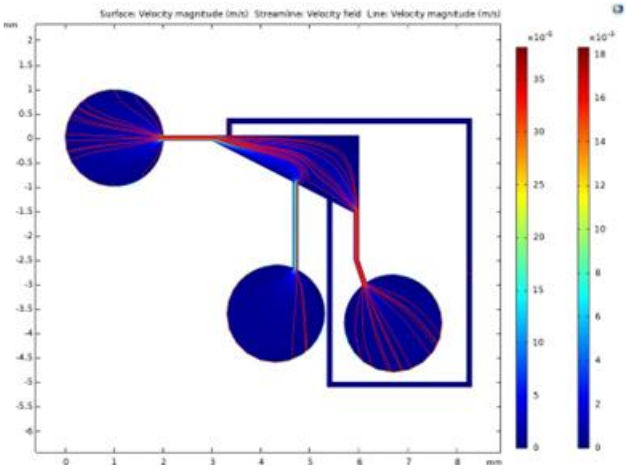

Figure 12 Streamline inside the tapered angle microfluidic for the first design

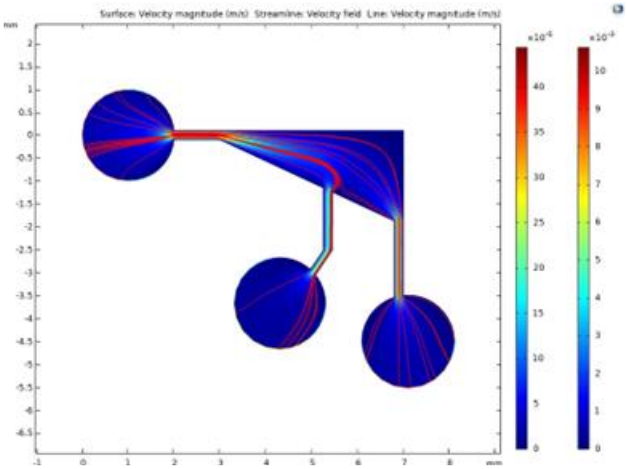

Figure 13 Streamline inside the tapered angle microfluidic for the first design

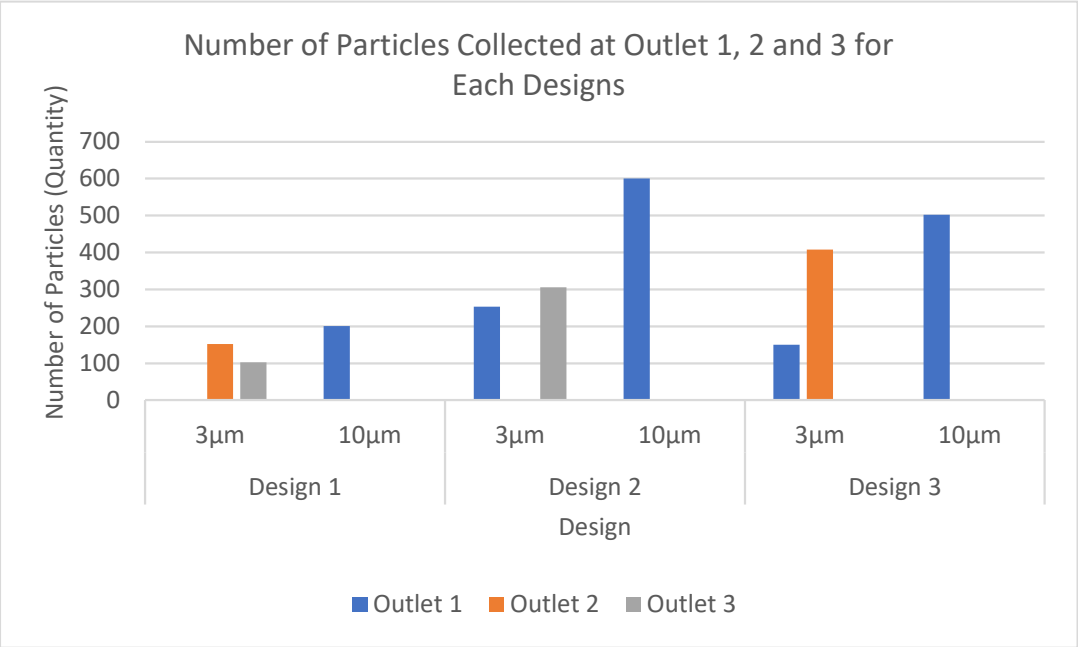

Figure 14 Particles collected on each outlet for each design

5.0 CONCLUSION

This study demonstrates the optimum designs of tapered angle microfluidics for particle separation based on the hydrodynamic principle. Numerous tapering angles and flow rates were employed in order to develop an optimal design. This yielded good outcomes. Utilizing the hydrodynamic principle and the sedimentation process, the device functions. The first design is capable of separating a mixture of PS microbeads of varying sizes and densities with a sample purity of one hundred percent at each outlet. Nonetheless, two designs were developed to improve the initial designs in terms of the number of particles captured at each outlet. The designs can achieve 100 percent sample purity of small particles at outlet 3, however, at outlet 1, the second and third designs achieve only 70 and 75 percent sample purity of large particles, respectively. Nevertheless, these devices are able to overcome the limits of previous cell separation devices based on hydrodynamic principles and have been demonstrated to be capable of separating a mixture of particles through the use of finite element simulation. In addition, the enhanced purity of the sample indicates that the proposed design might be used to create inexpensive and user-friendly microfluidic cell separation devices.

Conflicts of Interest

The author(s) declare(s) that there is no conflict of interest regarding the publication of this paper.

Acknowledgment

This project is supported by the Ministry of Higher Education of Malaysia and Universiti Teknologi Malaysia under the Professional Development Research University Grant [no. Q.J130000.21A2.06E67] in the project 'Development of Microfluidic Systems in PDMS for Microalgae Detection and Separation for Renewal Energy Application.

References

[1] B. Sutermaster and E. Darling. 2019. Considerations for Hhigh-yield, High-throughput Cell Enrichment: Fluorescence Versus Magnetic Sorting. *Scientific Reports.* 9(1). https://doi.org/10.1038/s41598-018-36698-1.

[2] Nitta, N., Sugimura, T., Isozaki, A., Mikami, H., Hiraki, K., Sakuma, S., … & Goda, K. 2018. Intelligent Image-activated Cell Sorting. *Cell.* 175(1): 266-276.e13. https://doi.org/10.1016/j.cell.2018.08.028.

[3] E. Llufrio, L. Wang, F. Naser, & G. Patti. 2018. Sorting Cells Alters Their Redox State and Cellular Metabolome. *Redox Biology*. 16: 381-387. https://doi.org/10.1016/j.redox.2018.03.004.

[4] T. Liu, W. Weng, Y. Zhang, X. Sun, & H. Yang. 2020. Applications of Gelatin Methacryloyl (gelma) Hydrogels in Microfluidic Technique-assisted Tissue Engineering. *Molecules.* 25(22): 5305. https://doi.org/10.3390/molecules25225305.

[5] Yu, M., Stott, S. L., Toner, M., Maheswaran, S., & Haber, D. A. 2011. Circulating Tumor Cells: Approaches to Isolation and Characterization. *Journal of Cell Biology*. 192(3): 373-382. https://doi.org/10.1083/jcb.201010021.

[6] T. Gorges, I. Tinhofer, M. Drosch, L. Röse, T. Zollner, T. Krahn*et al*. 2012. Circulating Tumour Cells Escape from Epcam-based Detection Due to Epithelial-to-mesenchymal

Transition. *BMC Cancer*. 12(1). https://doi.org/10.1186/1471-2407-12-178.
[7] J. Kaifi, M. Kunkel, D. Dicker, J. Joude, J. Allen, A. Das*et al*. 2015. Circulating Tumor Cell Levels are Elevated in Colorectal Cancer Patients with High Tumor Burden in the Liver. *Cancer Biology & Therapy*. 16(5): 690-698. https://doi.org/10.1080/15384047.2015.1026508.
[8] K. Bhargava, B. Thompson, & N. Malmstadt. 2014. Discrete Elements for 3d Microfluidics. *Proceedings of the National Academy of Sciences*. 111(42): 15013-15018. https://doi.org/10.1073/pnas.1414764111.
[9] A. Meer, K. Vermeul, A. Poot, J. Feijén, & I. Vermes. 2010. Flow Cytometric Analysis of the Uptake of Low-density Lipoprotein by Endothelial Cells in Microfluidic Channels. Cytometry Part A. 77A(10): 971-975. https://doi.org/10.1002/cyto.a.20937.
[10] S. Waheed, J. Cabot, N. Macdonald, T. Lewis, R. Guijt, B. Paull*et al*. 2016. 3d Printed Microfluidic Devices: Enablers and Barriers. *Lab on a Chip*. 16(11): 1993-2013. https://doi.org/10.1039/c6lc00284f.
[11] J. Qiu, Q. Gao, H. Zhao, J. Fu, & Y. He. 2017. Rapid Customization of 3d Integrated Microfluidic Chips via Modular Structure-based Design. *ACS Biomaterials Science Engineering*. 3(10): 2606-2616. https://doi.org/10.1021/acsbiomaterials.7b00401.
[12] Y. He, Y. Wu, J. Fu, Q. Gao, & J. Qiu. 2016. Developments of 3d Printing Microfluidics and Applications in Chemistry and Biology: A Review. *Electroanalysis*. 28(8): 1658-1678. https://doi.org/10.1002/elan.201600043.
[13] S. Şahin, C. Ünlü, & L. Trabzon. 2021. Affinity Biosensors Developed with Quantum Dots in Microfluidic Systems. *Emergent Materials*. 4(1): 187-209. https://doi.org/10.1007/s42247-021-00195-5.
[14] N. Yönet-Tanyeri, M. Amer, S. Balmert, E. Korkmaz, L. Falo, & S. Little. 2022. Microfluidic Systems for Manufacturing of Microparticle-based Drug-delivery Systems: Design, Construction, and Operation. *ACS Biomaterials Science Engineering,* 8(7): 2864-2877. https://doi.org/10.1021/acsbiomaterials.2c00066.
[15] X. Zhang, X. Xu, J. Wang, C. Wang, Y. Yan, A. Wu*et al*. 2021. Public-health-driven Microfluidic Technologies: From Separation to Detection. Micromachines. 12(4): 391. https://doi.org/10.3390/mi12040391.
[16] F. Zhang, L. Wu, W. Nie, L. Huang, J. Zhang, F. Li*et al*. 2019. Biomimetic Microfluidic System for Fast and Specific Detection of Circulating Tumor Cells. *Analytical Chemistry*. 91(24): 15726-15731. https://doi.org/10.1021/acs.analchem.9b03920.
[17] W. Tang, D. Jiang, Z. Li, L. Zhu, J. Shi, J. Yang*et al*. 2018. Recent Advances in Microfluidic Cell Sorting Techniques based on Both Physical and Biochemical Principles. Electrophoresis. 40(6): 930-954. https://doi.org/10.1002/elps.201800361.
[18] X. Zhang, X. Xu, J. Wang, C. Wang, Y. Yan, A. Wu*et al*. 2021. Public-health-driven Microfluidic Technologies: From Separation to Detection. Micromachines. 12(4): 391. https://doi.org/10.3390/mi12040391.
[19] Y. Wang, B. Nunna, N. Talukder, E. Etienne, & E. Lee. 2021. Blood Plasma Self-separation Technologies during the Self-driven Flow in Microfluidic Platforms. *Bioengineering*. 8(7): 94. https://doi.org/10.3390/bioengineering8070094.
[20] R. Nasiri, A. Shamloo, & J. Akbari. 2021. Design of a Hybrid Inertial and Magnetophoretic Microfluidic Device for CTCs Separation from Blood. *Micromachines*. 12(8): 877. https://doi.org/10.3390/mi12080877.
[21] Y. Song, D. Li, & X. Xuan. 2023. Recent Advances in Multimode Microfluidic Separation of Particles and Cells. *Electrophoresis*. 44(11-12): 910-937. https://doi.org/10.1002/elps.202300027.
[22] R. Nasiri, A. Shamloo, J. Âkbari, P. Tebon, M. Dokmeci, & S. Ahadian. 2020. Design and Simulation of an Integrated Centrifugal Microfluidic Device for CTCs Separation and Cell Lysis. *Micromachines*. 11(7): 699. https://doi.org/10.3390/mi11070699.
[23] N. Xiang and N. Zhang. 2022. Portable Battery-driven Microfluidic Cell Separation Instrument with Multiple Operational Modes. *Analytical Chemistry*. 94(48): 16813-16820. https://doi.org/10.1021/acs.analchem.2c03833.
[24] K. Matsuura and K. Takata. 2023. Blood Cell Separation using Polypropylene-based Microfluidic Devices based on Deterministic Lateral Displacement. *Micromachines*. 14(2): 238. https://doi.org/10.3390/mi14020238.
[25] A. Hochstetter, R. Vernekar, R. Austin, H. Becker, J. Beech, D. Fedosov*et al*. 2020. Deterministic lateral displacement: challenges and perspectives. *ACS Nano*. 14(9): 10784-10795. https://doi.org/10.1021/acsnano.0c05186.
[26] Y. Song, D. Li, & X. Xuan. 2023. Recent Advances in Multimode Microfluidic Separation of Particles and Cells. *Electrophoresis*. 44(11-12): 910-937. https://doi.org/10.1002/elps.202300027.
[27] J. Han, B. Krasniqi, J. Kim, M. Keckley, & D. DeVoe. 2020. Miniaturization of Hydrocyclones by High-resolution 3d Printing for Rapid Microparticle Separation. *Advanced Materials Technologies*. 5(4). https://doi.org/10.1002/admt.201901105.
[28] Z. Tian, C. Gan, L. Fan, J. Wang, & L. Zhao. 2022. Elastic-inertial Separation of Microparticle in a Gradually Contracted Microchannel. *Electrophoresis*. 43: 21-22, 2217-2226. https://doi.org/10.1002/elps.202200083.
[29] Z. Tian, C. Gan, L. Fan, J. Wang, & L. Zhao. 2022. Elastic-inertial Separation of Microparticle in a Gradually Contracted Microchannel. *Electrophoresis*. 43: 21-22, 2217-2226. https://doi.org/10.1002/elps.202200083.
[30] Sedimentation. BYJUS. 2016. [Online]. Available: https://byjus.com/chemistry/sedimentation/. [Accessed: 1-Jan-2022].
[31] I. L. Ahmad, M. R. Ahmad, M. Takeuchi, M. Nakajima, and Y. Hasegawa. 2017. Tapered Microfluidic for Continuous Micro-object Separation based on Hydrodynamic principle. *IEEE Trans. Biomed. Circuits Syst*. 11(6): 1413–1421.
[32] N. N. Yahya, N. A. Aziz, M. R. Buyong, and B. Y. Majlis. 2017. Size-based Particles Separation Utilizing Dielectrophoresis Technique. *2017 IEEE Regional Symposium on Micro and Nanoelectronics (RSM)*.
[33] N. A. Aziz, B. Bais, M. R. Buyong, B. Y. Majlis, and A. N. Nordin. 2015. Optimization of Focusing SAW Propagation in Piezoelectric Medium for Microfluidic Applications. *2015 Symposium on Design, Test, Integration and Packaging of MEMS/MOEMS (DTIP)*.